JOURNAL OF AGRICULTURAL AND FOOD CHEMISTRY
ARTICLE

J. Agric. Food Chem. **2010,** *58,* 1653–1663 **1653**
DOI:10.1021/jf903637s

Transcriptional Regulation and Molecular Characterization of the *manA* Gene Encoding the Biofilm Dispersing Enzyme Mannan *endo*-1,4-*β*-Mannosidase in *Xanthomonas campestris*

Yi-Min Hsiao*

Department of Medical Laboratory Science and Biotechnology, Central Taiwan University of Science and Technology, Taichung 406, Taiwan, Republic of China

Yu-Fan Liu

Department of Biomedical Sciences, Chung Shan Medical University, Taichung 402, Taiwan, Republic of China

Mei-Chiung Fang

Institute of Medical Biotechnology, Central Taiwan University of Science and Technology, Taichung 406, Taiwan, Republic of China

Yi-Hsiung Tseng

Institute of Microbiology, Immunology and Molecular Medicine, Tzu Chi University, Hualien 970, Taiwan, Republic of China

Exopolysaccharide and several extracellular enzymes of *Xanthomonas campestris* pv. campestris (Xcc), the causative agent of black rot in crucifers, are important virulence determinants. It is known that Clp (cAMP receptor protein-like protein) and RpfF (an enoyl-CoA hydratase homologue required for the synthesis of diffusible signal factor, DSF) regulate the production of these determinants. Addition of DSF or Xcc extracellular protein containing partially purified mannanase (EC 3.2.1.78, encoded by *manA*) can disperse the cell aggregates formed by *rpfF* mutant. In this study, nucleotide G 64 nt upstream of the *manA* translation start codon was determined as the transcription initiation site by the 5′ RACE technique. Transcriptional fusion assays showed that *manA* transcription is positively regulated by Clp and RpfF and induced by locust bean gum. The *manA* coding region was cloned and expressed in *E. coli* as recombinant ManA (rManA). The rManA was purified by affinity chromatography, and its biochemical properties were characterized. The rManA had a pH optimum at 7.0 (0.1 M Hepes) and a temperature optimum at about 37 °C. Sequence and mutational analyses demonstrated that Xcc *manA* encodes the major mannanase, a member of family 5 of glycosyl hydrolases. This study not only extends previous work on Clp and RpfF regulation by showing that they both influence the expression of *manA* in Xcc, but it also for the first time characterizes *Xanthomonas* mannanase at the protein level.

KEYWORDS: Transcriptional regulation; Clp; DSF; mannanase; *Xanthomonas*

INTRODUCTION

Xanthomonas campestris pv. campestris (Xcc) is a Gram-negative plant pathogenic bacterium causing black rot in crucifers, resulting in tremendous loss in agriculture (*1*). The ability of this organism to incite disease depends on several factors, such as the synthesis of large amounts of an exopolysaccharide and an array of extracellular enzymes (*2*−*4*).

The production of these virulence factors is positively regulated by a cell−cell communication mechanism through a small diffusible signal factor (DSF) (*5*, *6*), which has been identified as *cis*-11-methyl-2-dodecenoic acid (*7*). RpfF (an enoyl-CoA hydratase homologue) is required for the synthesis of DSF (*5*), while the RpfC/RpfG two-component system plays a role in DSF perception and signal transduction (*6*, *8*). A recent genetic and genomic analysis showed that the DSF signaling system regulates virulence gene expression through the global regulator Clp (cAMP receptor protein-like protein) (*9*).

Biofilms have been defined as matrix-enclosed bacterial populations that are adherent to each other and/or to surfaces or interfaces (*10*). The ability of plant pathogenic bacteria to form and disperse the biofilm may have implications for survival on

*To whom correspondence should be sent. Telephone: 886-4-2239-1647 ext. 6915. Fax: 886-4-2239-6761. E-mail: ymhsiao@ctust.edu.tw.

Published on Web 01/14/2010

Table 1. Primers Used in This Study

primer	sequence[a]	site[b]	direction and use[c]
−362*Pst*I	5′-CTGCAGGTGCCCATATCGGCCTCG-3′	−362	F, promoter analysis
−68*Pst*I	5′-CTGCAGCTGTACCTGTTGTCGGTTCT-3′	−68	F, complementation
+52XbaI	5′-TCTAGAACAAGGTGGACGCCGCAGAC-3′	+52	R, promoter analysis
+143*Sal*I	5′-GTCGACGGCTTGTCCGTGTCGGGC-3′	+143	F, overexpression, mutant construction, and confirmation
+1066NotI	5′-GCGGCCGCTCACTCCATCGCCCGC-3′	+1066	R, overexpression, mutant construction, and confirmation
+1067XbaI	5′-TCTAGAATCACTCCATCGCCCGCA-3′	+1067	R, complementation

[a] Added restriction sites are underlined. [b] Position of the 5′-end of the oligonucleotides relative to the transcription initiation site of the *manA* gene. [c] F, forward direction; R, reverse direction.

leaf surfaces and host plants, as well as on the spreading throughout the plant and the completion of the disease cycle (*11*). Recent works have indicated that the DSF signaling system is not only implicated in virulence factor production but is also involved in the regulation of biofilm dispersal in Xcc (*11*−*13*). Addition of DSF or an extracellular enzyme partially purified from the wild type disperses the biofilm formed by the *rpfF* mutant (*11*, *12*). Peptide mass fingerprinting and mutational analysis demonstrate that the enzyme responsible for this activity is mannanase (mannan *endo*-1,4-β-mannosidase, EC 3.2.1.78; also β-mannanase, *endo*-1,4-mannanase) (*12*).

To date, complete genomic sequences of three Xcc strains (ATCC33913, 8004, and B100) have been deposited in a public database (*14*−*16*). Only one mannanase gene (*manA*) has been annotated in these fully sequenced genomes of Xcc strains (*14*−*16*) as well as in strain Xc17, in which the genome sequence is almost complete (http://xcc.life.nthu.edu.tw). Although mannanases have been isolated from plants, fungi, and bacteria and many of the genes encoding the enzymes have been cloned and sequenced (*17*, *18*), to the best of our knowledge, there have been no detailed enzymatic studies of mannanase from *Xanthomonas* spp. It is only known that the *manA* mutant of Xcc strain 8004 has lost the mannanase activity and shown reduced virulence compared with the wild type (*12*). Neither the regulation of *manA* nor the characteristics of its coding product are clear. The aims of this study are to evaluate the transcriptional regulation of *manA*, to present the cloning and expression of *manA* and the purification and biochemical characterization of the produced recombinant ManA (rManA), as well as its effects on Xcc biofilm dispersal. This is the first study to characterize the mannanase gene expression in xanthomonads. Knowledge obtained from this study is expected to facilitate further investigations on the expression and function of mannanase in Xcc, as well as the understanding of the transcriptional regulation mechanisms of this phytopathogen.

MATERIALS AND METHODS

Bacterial Strains, Media, and Growth Conditions. *Escherichia coli* DH5α (*19*) and BL21(DE3) (Novagen) were the hosts for DNA cloning and recombinant protein expression, respectively. The Xcc strain Xc17 is a virulent wild-type strain isolated in Taiwan (*20*). Strains derived from Xc17 by marker exchange included the *clp* mutant AU56E (*21*), *rpfF* mutant RM17F (*22*), and *manA* mutant MG17. Luria−Bertani (LB) medium (*23*) was the general-purpose medium for cultivating *E. coli* and Xcc at 37 and 28 °C, respectively. The XOLN medium contained basal salts, 0.0625% tryptone, and 0.0625% yeast extract (*24*). Glycerol (2%) and locust bean gum (LBG, 0.5%, Sigma-Aldrich) were supplemented as required. Antibiotics were added when necessary: ampicillin (50 μg/mL), kanamycin (50 μg/mL), gentamycin (15 μg/mL), and tetracycline (15 μg/mL). Liquid cultures were shaken at 220 rpm. Solid media contained 1.5% agar.

DNA Techniques. Enzymes were purchased from Promega, Takara, and Roche. Standard protocols including the conditions used for plasmid DNA extractions, restriction endonuclease digestions, agarose gel electrophoresis, and isolation and ligation of DNA fragments have been described elsewhere (*25*). PCR was carried out as previously described (*26*) using the primers listed in **Table 1**. DNA sequences on both strands were determined by the dideoxy chain termination method (*27*). Transformation of *E. coli* was performed by the standard method (*25*) and that of Xcc by electroporation (*28*).

Mapping of the 5′-End of the *manA* mRNA. The 5′ RACE (rapid amplification of cDNA ends) system (*29*) was used to determine the transcription initiation site using the Invitrogen Version 2.0 kit (Invitrogen). Total RNA was isolated from Xc17 (midexponential phase) by the Qiagen RNA extraction system (Qiagen Rneasy Mini Kit). The Abridged Anchor Primer (AAP) and Abridged Universal Amplification Primer (AUAP) were used in combination with the gene-specific primers. The gene-specific primers for RT-PCR, nested PCR1, and nested PCR2 were 900R (complementary to *manA* nt 449−468, 5′- GCCGAAGGGC-TCGTTGCCGA-3′), 771R (complementary to *manA* nt 420−439, 5′-GGTGTCGTGCACCTCCAGCA-3′), and 621R (complementary to *manA* nt 170−189, 5′-CAGCGCGGCATCAGTGCGAT-3′), respectively. The PCR products were ligated into the yT&A vector (Yeastern), which contained the M13 forward and reverse primers for sequence verification.

Transcriptional Fusion Assay. The *manA* upstream region was cloned into the *Pst*I-*Xba*I sites upstream of the promoter-less *lacZ* gene in the promoter-probing vector pFY13−9 (*30*). Construct pFY−362+52, which carried nt −362/+52 regions relative to the *manA* transcription initiation site, was introduced into different Xcc strains by electroporation. Strains harboring this construct were grown overnight and inoculated into fresh media to obtain an initial OD_{550} of 0.35, after which growth was allowed to continue. Samples were taken in triplicate at designated intervals and the β-galactosidase activity was assayed as previously described, with the enzyme activity expressed in Miller units (*23*).

Mannanase Activity Analysis. Qualitative evaluation of extracellular mannanase activity was performed on agar plates containing LBG substrate as previously described (*31*) with some modification. Strains to be assayed were grown overnight in LB medium and diluted with sterile distilled water to $OD_{550} = 1$. Then, 3 μL was deposited onto the surface of the LB plates containing 0.2% LBG. After 2 days of incubation, the plates were stained with 0.2% Congo red for 1 h and destained with 1 M NaCl for 30 min. Polymer degradation by manannase depleted the plate of stain-binding material, forming clearing zones. Quantitative assay of mannanase activity was carried out by monitoring the hydrolysis of azo-carob galactomannan (ACG, Megazyme) substrate (*32*). The ACG is a derivative of LBG to which a dye, Remazol Brilliant Blue R, has been covalently bound to the galactomannan polymannose backbone at an average of 1 of every 20 mannose units. Digestion of the substrate by mannanase breaks the mannose chain, releasing smaller, more soluble galactomannan pieces, which, because of the chromogenic dye, can be monitored spectrophotometrically. The assay was performed as follows. A 0.4 mL portion of a 1% solution of ACG in 0.1 M Hepes (pH 7.0) was added to a 1.5 mL microcentrifuge tube. The reaction was started by adding 0.2 mL of an enzyme sample to the tube placed in a 37 °C water bath. After a 30 min incubation, the reaction was stopped by placing the tubes in ice. The nondegraded substrate was precipitated at room temperature for 5 min by adding 0.6 mL of 95% ethanol. After centrifugation at 10000 g for 5 min, the increase in absorbance of the supernatant was measured at 595 nm and compared with that of a blank run under the same conditions. One unit of activity for assay with this substrate was defined as the amount of enzyme that increased the absorbance by 1 unit in 1 min.

Overexpression and Purification of rManA Protein. Plasmid pETmanA was constructed by inserting the 924 bp Xc17 *manA* coding

Figure 1. (**A**) Mapping of the 5′-end of the Xcc *manA* transcript by the 5′ RACE method. The *manA* upstream region (−64 to +189 relative to the *manA* start codon) was PCR-amplified using AUAP in combination with gene specific primer 621R (lane 2). Lane 1 contained molecular size markers. (**B**) Sequence of the *manA* upstream region. Shown are +1 (the determined transcription initiation site), predicted −10/−35 sequences, putative ribosomal binding site (RBS), start codon (ATG), and position of 621R.

region into the *Sal*I-*Not*I sites of expression plasmid pET30b (Novagen) that had been digested with the same enzymes. This construct encoded the complete ManA without the signal peptide plus 56 amino acids at the N-terminus and with six histidine residues to facilitate purification. *E. coli* BL21(DE3)(pETmanA) was grown in the LB broth until an OD_{595} of 0.5−0.6 was reached. At this point, protein production was induced by the addition of isopropyl thio-β-D-galactoside (IPTG) to a final concentration of 1 mM. The rManA was purified from the crude extracts prepared from a 50 mL culture using Bug-Buster protein extraction reagent and the His-Bind affinity column (Novagen). Protein purity was checked by SDS−PAGE followed by Coomassie blue staining of the protein bands (*33*). The purified protein was dialyzed against 1 L of dialysis buffer (50 mM potassium phosphate, pH 7.0 containing 0.5 M KCl, 1 mM EDTA, 0.2 mM dithiothreitol, and 5% glycerol) at 4 °C with three changes of the buffer. The protein was then concentrated with a Microcon-10 centrifugal filter device (Millipore) and stored in aliquots in 50% (v/v) glycerol at −20 °C until use. Protein contents were determined by the method of Bradford (*34*) using protein assay reagent purchased from Bio-Rad Laboratories (Hercules) with BSA as the standard.

Zymography. After electrophoresis was completed, SDS was removed from the gel by washing three times for 1 h in 10 mM Hepes buffer (pH 7.0) at room temperature on a slowly rotating platform shaker. Activity detection of mannanase in the polyacrylamide gel was done by overlay on an agar sheet (1.5 mm thick) containing 0.2% LBG and 0.1 M Hepes buffer (pH 7.0) on the gel for 30 min at room temperature. The agarose gel sheet was dipped into 0.2% Congo red solution and stained for 30 min. The Congo red was poured off, and the gel sheet was washed with 1 M NaCl until excess stain was removed. The band corresponding to mannanase appeared as a clear zone on a red agar sheet after staining with 0.2% Congo red solution.

Effect of pH and Temperature. The optimum pH for rManA activity was determined at 37 °C at various pH values in 0.1 M sodium acetate (pH 5, 5.5, and 6) and 0.1 M Hepes (pH 6, 7, 8, and 9). The optimum temperature for rManA activity was determined by assaying the enzyme at various temperatures ranging from 25 to 50 °C.

Thermal Stability. Thermal inactivation of the rManA was determined by incubating the purified enzyme for 10 min at various temperatures ranging from 4 to 60 °C, cooling it to room temperature for 5 min, and then assaying for residual activity. Purified rManA was stored at room temperature, and the change in activity was measured at timed intervals to determine the storage stability.

Metal Ion and Chemical Reagent Effects of rManA Activity. The purified rManA protein was first dialyzed three times in buffer containing 20 mM Hepes (pH 7.0) before addition of various metal ions and chemical reagents. The activity assay was performed as previously described.

Enzyme Kinetics of rManA. The maximum velocities (V_{max}) and the Michaelis constants (K_m) were determined according to a Lineweaver−Burk plot. All reactions were carried out in triplicate.

Construction of *manA* Mutant. A *manA* mutant was constructed by insertional mutation of Xc17 and designated as MG17. The 924 bp *Sal*I-*Not*I fragment containing the Xc17 *manA* gene was cloned in the *E. coli* vector pOK12 (*35*), which contained P15A *ori* and could not be maintained in Xcc, giving pOKmanA. A Gm^r cartridge from pUCGM (*36*) was inserted into the unique *Hin*cII site within the pOKmanA insert. The resultant plasmid, pOKmanAG, was electroporated into Xc17, allowing for double crossover via homologous recombination through the identical regions in the chromosome and the plasmid to replace the wild-type sequence. Insertion of a Gm^r cartridge into *manA* was confirmed by PCR.

Complementation of *manA* Mutant. Plasmid pRKmanA was generated by cloning the 1135 bp DNA fragment encompassing the upstream 132 bp plus the entire coding region of the Xc17 *manA* into the *Pst*I-*Xba*I sites of the broad-host-range vector pRK415 (*37*). This construct contained the *manA* gene in the downstream orientated in the same direction as the *lac* promoter.

Western Blotting. Xc17, its *manA* mutant MG17, and the complement strain MG17(pRKmanA) were analyzed by Western blotting to detect the ManA protein produced, using purified rManA as positive control. The culture conditions were the same as those of promoter analysis to obtain an initial OD_{550} of 0.35. After 24 h, samples were taken and subjected to Western blot analysis. Briefly, a similar amount of culture supernatant from each strain was separated by SDS−PAGE and transferred electrophoretically to a polyvinylidene difluoride membrane and then probed with mouse anti-rManA serum which was produced by injecting the pET-expressed rManA protein into BALB/c mice followed by rabbit antimouse IgG horseradish peroxidase conjugate. Positive bands were detected with the ECL reagents as recommended by the supplier (Amersham).

Sequence Alignment and Homology Modeling. Multiple sequence alignment of selected β-mannanase proteins was generated with the ClustalX package using a standard PAM (Point Accepted Mutation) series protein weight matrix. Secondary structure alignment was assigned on the basis of the detection of hydrogen bonds defined by an electrostatic criterion using the Dictionary of Protein Secondary Structure database (DSSP) method obtained from PDBsum database. The 3-dimensional structure of Xcc ManA was built by homology modeling using the ModBase standard process. The template protein was *Thermomonospora fusca* β-mannanase (PDB code 1BQC), in which 47% identity is shared with Xcc ManA. The dataset is TIMbarrel_templates, and the Modpipe version is 1.0. Figures were drawn with the program AccylyrsTM Viewer-Lite 4.2.

RESULTS

Mapping of the 5′-End of the *manA* Transcript. To identify the Xcc *manA* transcription initiation site, the 5′ RACE method was employed. In 5′ RACE experiments, sequencing of the fragment generated by nested PCR (289 bp) showed that nucleotide G, 64 nt upstream from the translation start codon, was the transcription initiation site of *manA* (**Figure 1**).

Expression of *manA* Requires Clp and RpfF and Is Induced by LBG. To characterize the expression of *manA*, the upstream region of *manA* was PCR-amplified and cloned into the promoter-probing vector pFY13−9 with *lacZ* as the reporter, giving rise to

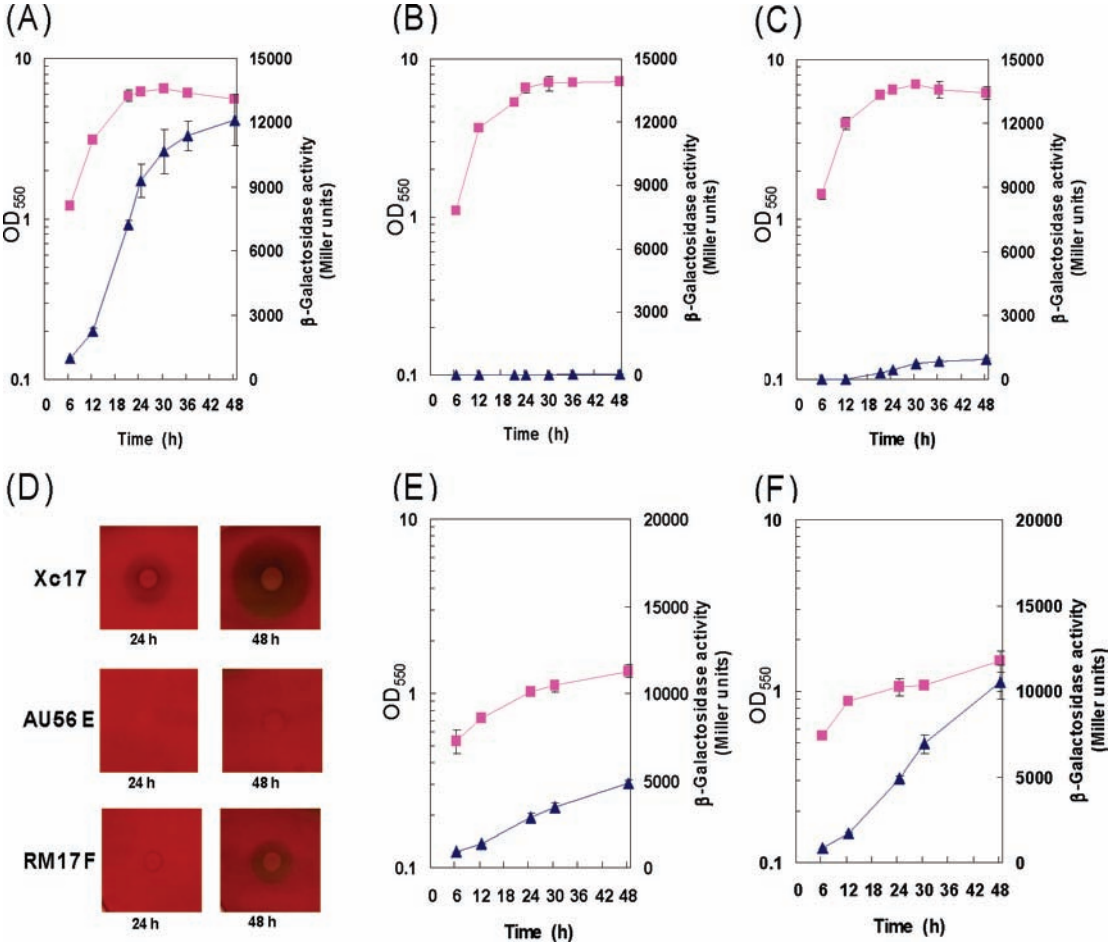

Figure 2. (**A**−**D**) Effects of *clp* and *rpfF* mutations on *manA* expression. (**A**−**C**) Levels of β-galactosidase (triangles) as a function of cell growth (squares) in Xc17 (**A**), AU56E (**B**), or RM17F (**C**) containing pFY−362+52. The experiments were repeated three times for each strain. (**D**) Detection of extracellular mannanase activity in wild-type Xc17 (upper), *clp* mutant AU56E (middle), and *rpfF* mutant RM17F (bottom). The mannanase activity was evaluated using LB medium supplemented with LBG at 24 and 48 h. Clearing zones were visualized after Congo red staining. Consistent results were obtained from three experiments with triplicate samples. (**E** and **F**) Levels of β-galactosidase (triangles) as a function of cell growth (squares) in Xc17(pFY−362+52). Cells were grown in the XOLN medium containing glycerol as carbon source with (**F**) or without (**E**) LBG. The experiments were repeated three times for each strain.

transcriptional fusion pFY−362+52, as described in the Materials and Methods. The resultant plasmid was electroporated separately into the wild type Xc17 and its *clp* mutant AU56E and *rpfF* mutant RM17F. Strains containing pFY−362+52 were used to assay for *manA* promoter activity, and samples were taken at intervals to measure β-galactosidase activity.

Xcc strains harboring pFY−362+52 grew at similar rates (**Figure 2A**−**C**) and reached about the same final yields (about 6.4 of OD_{550}), suggesting that neither mutation in *clp*/*rpfF* nor the presence of the plasmid affects their growth in the LB medium used here. The promoter activities in AU56E(pFY−362+52) (**Figure 2B**) and RM17F(pFY−362+52) (**Figure 2C**) were lower (42 U and 927 U) than those expressed by Xc17(pFY−362+522) (**Figure 2A**), 12137 U, at 48 h. In terms of translation, the *clp* mutant (AU56E) formed no significant clearing zones, whereas the *rpfF* mutant (RM17F) gave significantly smaller clearing zones using wild type Xc17 for comparison in the LBG containing plate (**Figure 2D**).

The *manA* promoter activity in Xc17(pFY−362+52) was also determined when cells were grown in XOLN containing glycerol with or without LBG. No significant differences in growth rates or final yields were observed between the strains when the cells were grown under the same conditions (**Figure 2E** and **F**). In the presence of LBG, the β-galactosidase level expressed in Xc17-(pFY−362+52) increased following growth and reached 10506 U (**Figure 2F**), a similar level to that detected in the same cells grown in LB after 48 h (**Figure 2A**). Without LBG, only 4805 U was produced (**Figure 2**E).

Production and Molecular Characterization of the rManA Protein. In order to investigate the biochemical characteristics of the product encoded by *manA*, it was overexpressed in the *E. coli*, as outlined in the Materials and Methods. As shown in **Figure 1B**, a putative ribosomal binding site (GGAG) was present 7 nt upstream of the Xcc *manA* start codon. It encoded a protein of 333 amino acids (including the putative signal peptide) with a calculated molecular mass of 35699 Da and a p*I* of 7.83. As a secreted protein, it had an N-terminal putative signal sequence of 26 amino acids with a possible cleavage site (AHA^{26}-$G^{27}L$), as predicted by Signal P software (*38*). Concerning the extracellular location, the Xcc *manA* coding region without the predicted signal peptide was amplified by PCR, and the resulting 924 bp fragment was cloned into pET30b between *Sal*I and *Not*I sites and subsequently transformed into *E. coli* BL21(DE3) for rManA production. As a consequence of using these cloning sites, the resulting protein would have 56 additional amino acid residues at the N-terminus of the wild-type protein.

Compared with protein samples before IPTG addition, upon induction with IPTG for different times, a 42-kDa protein band was produced (**Figure 3A**, lanes 1−4). Cell-free extracts from cultures treated with IPTG for 2 h were harvested for protein

purification using a His-Bind affinity column and elution with imidazole. SDS−PAGE analysis of the affinity-purified protein revealed a homogeneous protein with a molecular mass of approximately 42 kDa (**Figure 3A**, lane 5), which is close to the predicted molecular mass (encoded by the 924 bp PCR amplified *manA* fragment plus the extra N-terminal 56 amino acids encoded by pET30b). Zymography of the purified rManA also displayed an active band (**Figure 3B**) with similar size, as shown in SDS-PAGE.

Biochemical Characterization of rManA. The rManA was shown to have a pH optimum of about pH 7.0 (**Figure 4A**) and a temperature optimum of about 37 °C (**Figure 4B**). It retained only 48.89% and 65.40% of its maximal activity at pH 5 and pH 9, respectively. While at 25 and 50 °C, only 82.60% and 45.16% of its maximal activity was detected, respectively. Thus, rManA activity assays were performed at pH 7.0 and 37 °C. Irreversible denaturation of rManA mainly occurred at above 50 °C, indicated by the dramatically decreased mannanase activity when the enzyme was incubated at or above 50 °C (**Figure 4C**). The rManA can be stored at room temperature without significant loss of activity after one month (**Figure 4D**).

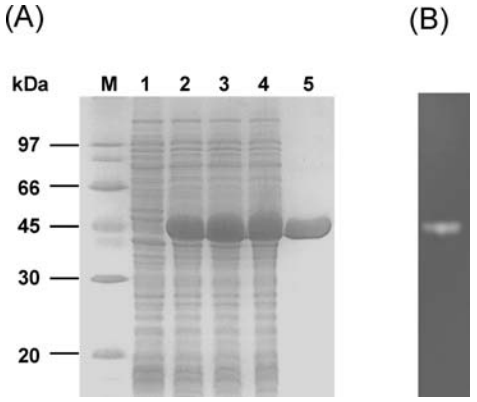

Figure 3. (**A**) SDS-PAGE analysis of rManA. *E. coli* BL21(DE3)-(pETmanA) in the midlog phase was induced with IPTG, and cell lysate was separated by SDS-PAGE following Coomassie brilliant blue staining. Lane M is molecular weight markers. Induction times were 0, 2, 3, and 4 h (lanes 1, 2, 3, and 4). Lane 5 was purified rManA from affinity chromatography. (**B**) Zymography. Purified rManA was separated by SDS-PAGE, followed by activity staining with LBG as substrate.

Purified rManA was incubated with various cations (1 mM) or chemical reagents at 37 °C for 30 min, and then residual mannanase activities were assayed by the standard method. As shown in **Table 2**, the activity was slightly enhanced by Na^+, K^+, Ca^{2+}, Mg^{2+}, and Mn^{2+}. The mannanase activity was inhibited moderately by Fe^{2+}, Al^{3+}, and Fe^{3+} and strongly inhibited by Ag^+, Cu^{2+}, Zn^{2+}, and Hg^{2+}. The activity of rManA was not affected by EDTA and iodoacetic acid at 10 mM and 1 mM concentrations (**Table 2**). The rManA was also resistant to the reducing agents β-mercaptoethanol and dithiothreitol and to the detergents Tween 20 and Triton X-100.

Kinetic studies determined the affinity of rManA for its substrate azo-carob galactomannan (ACG). The K_m value was 0.88 mg/mL. The hydrolyzing efficiency of rManA for the substrate, as indicated by its V_{max} value, was 282.55 U/(min mg).

ManA is the Major Mannanase Responsible for LBG Hydrolysis in Xcc. To explore the physiological role of *manA*, the *manA* mutant (MG17) was constructed by insertional mutation (see Materials and Methods for details). *manA* is flanked by genes that are transcribed in the opposite orientation in the Xcc genome; hence, disruption of *manA* does not have polar effects. Simultaneously, a complemented strain, named MG17(pRKmanA), was also created by introducing the *manA*-expression plasmid pRKmanA into the mutant strain MG17.

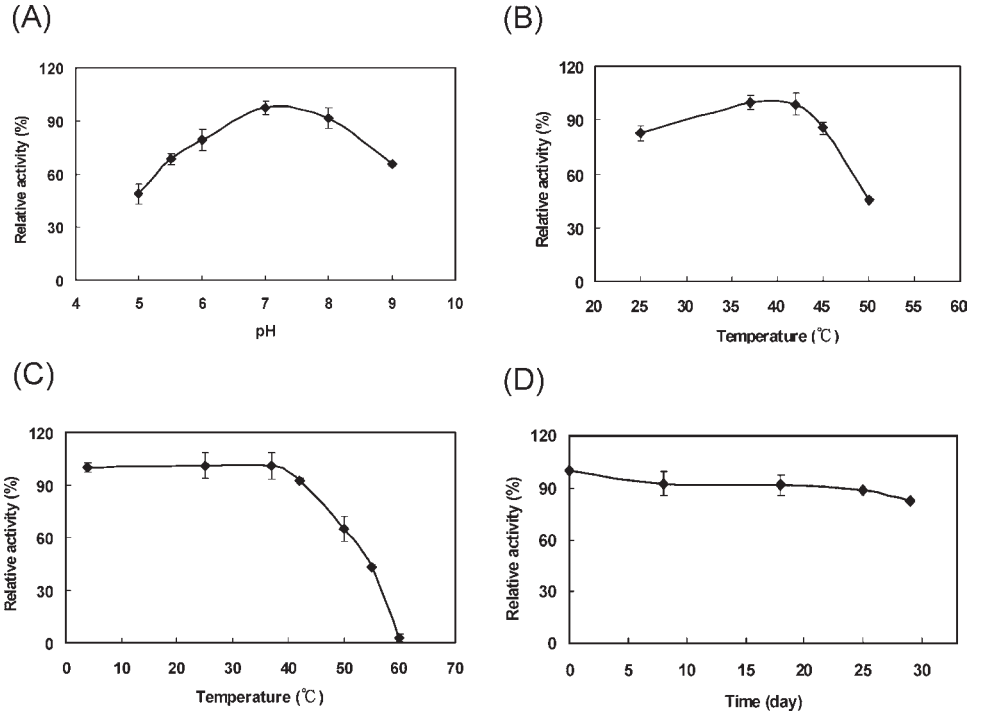

Figure 4. (**A**) pH activity profiles of purified rManA. The buffers used were 0.1 M sodium acetate (pH 5.0−6.0) and 0.1 M Hepes (pH 6.0−9.0). (**B**) Temperature activity profiles of purified rManA. The enzyme activities were assayed at various temperatures in 0.1 M Hepes buffer (pH 7.0). (**C**) Thermal stability of purified rManA. The enzyme was preincubated at various temperatures, as indicated for 10 min, and the residual activities were determined. (**D**) Storage stability of rManA. The purified rManA was stored at room temperature; the change in activity was measured at timed intervals to determine the storage stability. The activities in each above test were expressed as a percentage of the maximal activity, and the results are the means of three replications.

To clarify whether a mutation in *manA* has any effect on bacterial growth, the growth rates of the wild type Xc17, *manA* mutant MG17, and complemented strain MG17(pRKmanA) were compared. As shown in **Figure 5A**, these strains grew at comparable rates and reached similar final OD_{550} values in LB (6.31−6.66) after entering stationary phase, indicating that a mutation in *manA* does not affect the growth of Xcc in LB media. In a preliminary experiment, the MG17 exhibited significantly reduced mannanase activity compared with Xc17 on plate assay using LBG as substrate (data not shown). Also shown in **Figure 5A**, no mannanase activity was detected in *manA* mutant on quantitative assay when compared with the wild type at the times indicated. The extracellular mannanase activity in Xc17 increased following cell growth and reached a maximum at 48 h (212 mU/OD_{550}). The course of increase was similar to that seen on *manA* promoter activity assay (**Figure 2A**). Complementation of the mutant MG17 by *in trans* expression of wild-type *manA* not only restored the production of mannanase to the wild-type level but also gave a higher activity (3622 mU/OD_{550}) than that of the wild type strain (**Figure 5A**).

Table 2. Effects of Metal Ions and Chemical Reagents on rManA Activity

	residual activity (%)
metal ions (1 mM)	
none	100
NaCl	113
KCl	114
$AgNO_3$	18
$CaCl_2$	119
$MgCl_2$	118
$MgSO_4$	112
$MnCl_2$	109
$FeSO_4$	59
$CuCl_2$	1
$CuSO_4$	2
$ZnCl_2$	16
$HgCl_2$	1
$AlCl_3$	31
$FeCl_3$	37
reagents	
EDTA (10 mM)	110
iodoacetic acid (1 mM)	107
β-mercaptoethanol (1 mM)	121
dithiothreitol (1 mM)	114
Tween 20 (1%)	117
Triton X-100 (1%)	123

Immunoblot analysis of extracellular proteins of Xc17 and MG17(pRKmanA) with polyclonal antibody against purified rManA also detected a single band with a molecular mass of approximately 33 kDa (**Figure 5B**, lanes 1 and 3). This is in agreement with the predicted molecular mass of ManA according to the amino acid sequence after signal sequence cleavage (33129 Da) and consistent with an extracellular location in Xcc. No ManA protein was detected in *manA* mutant MG17 (**Figure 5B**, lane 2). The results of Western blot analysis agreed with the observations of no clear zone on LBG plate assay (data not shown) and no activity on mannanase quantification analysis (**Figure 5A**) for *manA* mutant compared with its wild type strain. These results imply that ManA is the major mannanase to metabolize LBG of Xcc.

ManA Is Similar to Other Mannanases Belonging to Family 5 of the Glycosyl Hydrolases. Xcc ManA showed 78 and 77% identities with the putative *endo*-1,4-β-mannosidase (XCV1826) of *X. campestris* pv. vesicatoria strain 85-10 (Gene code *XCV1826*) (*39*) and the mannan *endo*-1,4-β-mannosidase (XAC1796) of *X. axonopodis* pv. citri strain 306 (Gene code *XAC1796*) (*16*), respectively. It also shared over 50% identity with the homologous members of family 5 of the glycosyl hydrolases (GH) (*40*) from other bacteria such as the *endo*-1,4-β-mannanase 5A (Man5A) of *Cellvibrio japonicus* (59%), the *endo*-1,4-β-mannanase 5B (Man5B) of *Cellvibrio japonicus* (54%), the mannan *endo*-1,4-β-mannosidase (ManA) of *Streptomyces lividans* (54%), and the β-1,4-mannanase (ManA) of *Vibrio* sp. MA-138 (53%) (*41*−*43*). The accession numbers of the above-mentioned mannanases are listed in **Table 3**.

So far the crystal structures of three bacterial mannanases belonging to GH5 have been determined and deposited in the Protein Data Bank database: *T. fusca* β-mannanase (Tfu Man, PDB code 1BQC) (*44*); *Bacillus* sp. strain JAMB-602

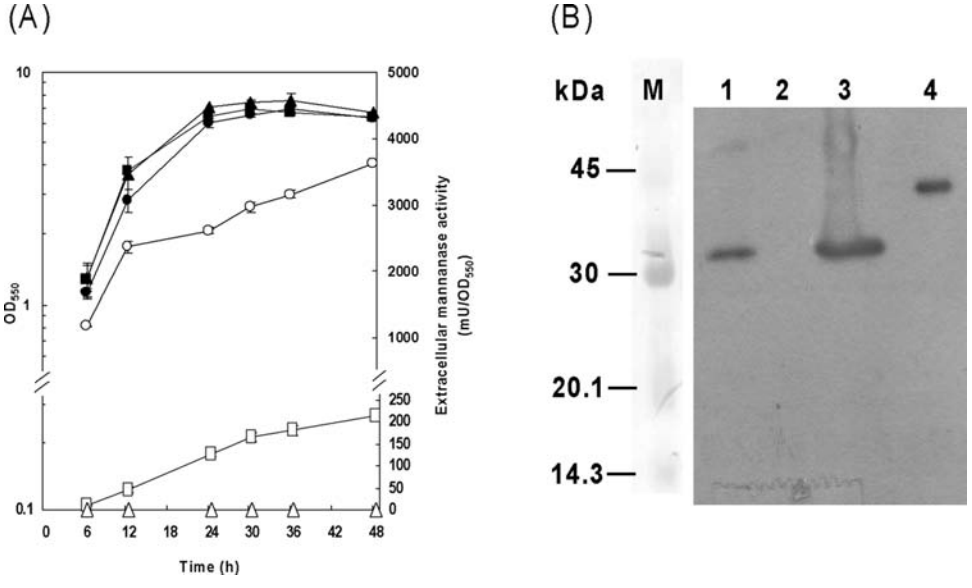

Figure 5. (**A**) Quantification of the mannanase activity in the supernatant of wild-type Xc17 (■, □), *manA* mutant MG17 (▲, △), and complemented strain MG17(pRKmanA) (●, ○). Cells were grown in LB medium, and samples were taken at intervals for measurements of OD_{550} (■, ▲, ●) and mannanase activity (□, △, ○). The experiments were repeated three times for each strain. (**B**) Western blot analysis of extracellular proteins from Xc17 (lane 1), MG17 (lane 2), MG17(pRKmanA) (lane 3), and purified rManA (lane 4) with polyclonal anti-rManA serum. Lane M is rainbow molecular weight markers.

Table 3. Comparison of the Sequences and Characteristics of Xcc ManA and Reported Mannanases from the GH5 Family

organism	protein (amino acids)	accession no.	mannanase domain	additional domain	optimal pH	optimal temperature	ref
X. campestris pv. campestris	ManA (333)	NP_637144	34-287	none	7.0	37 °C	*16* and this study
X. campestris pv. vesicatoria	XCV1826 (325)	YP_363557	34-284	none	ND[a]	ND	*39*
X. axonopodis pv. citri	XAC1796 (328)	NP_642123	37-287	none	ND	ND	*16*
Cellvibrio japonicus	Man5A (430)	AA031759	58-277	CBM10: 360−389, 395−422	7.5−8.0	ND	*43*
Cellvibrio japonicus	Man5B (561)	AA031760	32-285	CBM10: 369−396; CBM2a: 464−560	7.5−8.0	ND	*43*
Streptomyces lividans	ManA (383)	P51529	45-292	CBM10: 346−376	6.8	58 °C	*41*
Vibrio sp. MA-138	ManA (395)	BAA25188	28-279	CBM10: 325−359	6.5	40 °C	*42*
Vibrio sp. MA-138	Man5C (669)	BAG69482	50-351	CBM27: 499−666	7.0	50 °C	*17*

[a] ND, not determined.

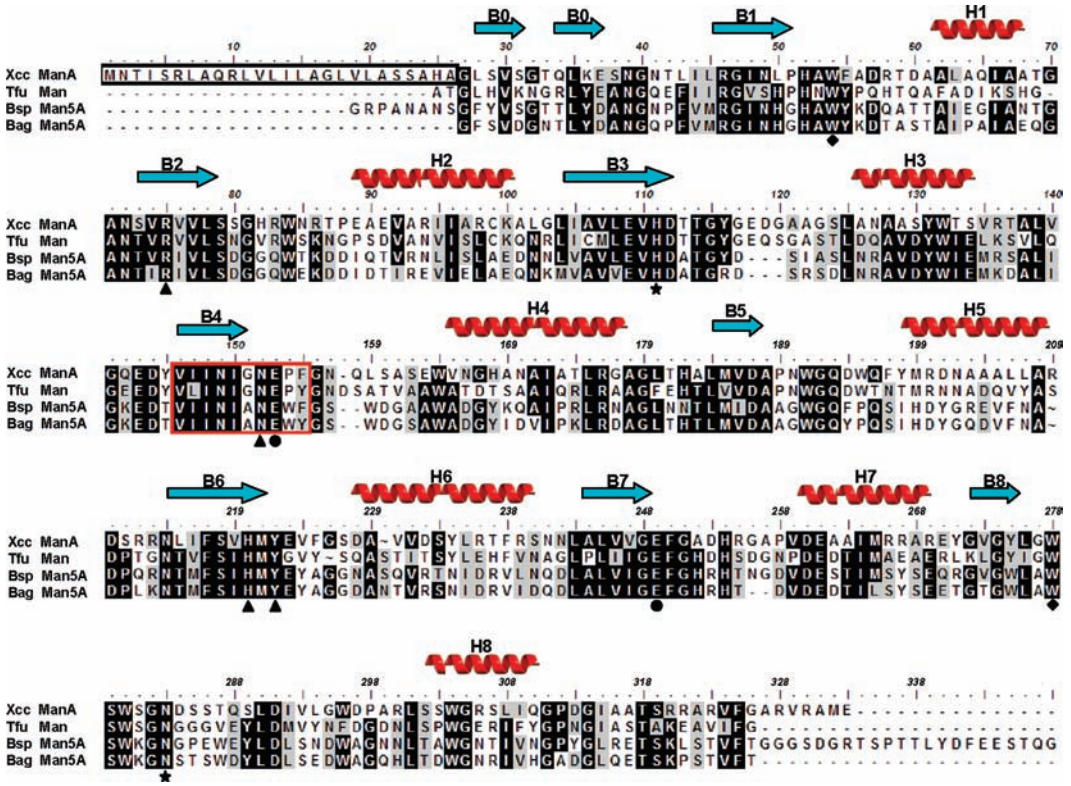

Figure 6. Schematic presentation of sequence and secondary structure alignment to predict the functional amino acids of Xcc ManA. The sequences are as follows: Xcc ManA, Xcc β-mannanase (GenBank accession no. NP_637144); Tfu ManA, *T. fusca* β-mannanase (PDB code 1BQC); Bsp ManA, *Bacillus* sp. strain JAMB-602 β-mannanase (PDB code 1WKY); and Bag Man5A, *B. agaradhaerens* β-mannanase (PDB code 2WHL). Identical amino acids are revealed by black shading and similar amino acids by gray shading. Signal peptide and GH5 family signature sequences are highlighted in black and red boxes, respectively. Secondary-structure alignment of the enzymatic catalysis domain is shown above the sequences. Numbering above the sequence corresponds to Xcc ManA. Asterisks denote residues that involve substrate recognition; filled circles mark catalytic proton donor and nucleophile residues; triangles indicate residues involved in stabilizing the catalytic site environment via functional group interactions; diamonds reveal the substrate stacking hydrophobic platforms.

β-mannanase (Bsp Man5A, PDB code 1WKY) (*45*); and *B. agaradhaerens* β-mannanase (Bag Man5A, PDB code 2WHL) (*46*). Multiple sequence alignment of Xcc ManA and the catalytic domain of these three mannanases indicated that Xcc ManA shares 47, 43, and 41% identities with them, respectively (**Figure 6**). Eight conserved residues in GH5 enzymes have been demonstrated to be responsible for the catalytic activity of the enzymes (*47*). They are well conserved in the above-mentioned mannanases and are situated at Arg^{75}, His^{111}, Asn^{152}, Glu^{153}, His^{220}, Tyr^{222}, Glu^{249}, and Trp^{278} in Xcc ManA (**Figure 6**).

DISCUSSION

Upstream Region of *manA*. The *manA* gene was flanked by the upstream *XCC1777* (1857 bp encoding a hypothetical protein) and the downstream *XCC1779* (576 bp encoding a two-component system regulatory protein), both in the opposite direction as *manA*, with intergenic regions of 426 and 321 bp, respectively (*16*). Due to its orientation and long intergenic regions with flanking genes, Xcc *manA* is likely to be a monocistronic gene that possesses its own promoter.

The 5′ noncoding region of the sequence does not contain a strong *E. coli* promoter. The consensus promoter sequence for *Xanthomonas* is not well-defined. Two conserved regions around −35 and −10 are TTGTNN and (T/G)ATNA(A/T), which are separated by 17−43 bp (*48*). As predicted, the −35/−10 regions of CTGTGA/TTGGCA, with 5/6 and 3/6 bases matching (underlined bases) the consensus sequence of *Xanthomonas* (*48*), were located at −45/−11 (with a spacer of 28 nt) relative to the determined *manA* transcription initiation site (**Figure 1B**). The distance between the transcription initiation site and the −35/−10 box is longer than that normally seen in bacteria, while the spacer of the −35/−10 regions is within the range predicted in *Xanthomonas* (*48*).

Transcriptional Regulation of *manA*. In Xcc, Clp and RpfF/DSF positively regulate the expression of several extracellular

enzymes. Mutation in *clp* causes pleiotropic effects, including drastic reduction in the production of exopolysaccharide and extracellular enzymes, as well as loss of virulence and sensitivity to filamentous phage ϕLf (*21*, *30*, *49*). Gel retardation and transcriptional fusion assays have shown that Clp exerts a positive control over expression of *engA* (encoding major endoglucanase), *pehA* (encoding major polygalacturonase), and *pelA1* (encoding major pectate lyase) by direct binding to the upstream Clp-binding sites, while *prt1* (encoding the major protease) without a Clp-binding site is controlled in an indirect manner (*22*, *26*, *50*, *51*). Addition of DSF to an *rpfF* mutant can phenotypically restore the production of extracellular endoglucanase and pectate lyase (*5*). Transcriptional fusion assays have shown that RpfF positively regulates *pehA* and *pelA1* transcription (*22*, *50*).

In this study, the promoter activity of *manA* is significantly lower in *clp* mutant (0.35%) and *rpfF* mutant (7.64%) compared with the case of the wild type strain revealed in the transcriptional fusion assay (**Figure 2A**−**C**). In addition, the results on mannanase activity assays also shown consistent outcomes (**Figure 2D**). These data indicated that Clp and RpfF are required for expression of the *manA* gene in Xc17. The DNA sequence for Clp binding has been evaluated and found to be similar to that of the *E. coli* CRP-binding site (5′-AAATGTGA-TCTAGA-TCA-CATTT-3′) (*52*). However, no sequences showing similarity to the conserved Clp-binding site were found in the *manA* promoter region (**Figure 1B**). Therefore, it is reasonable to predict that a regulatory protein of which expression requires the function of Clp regulates the *manA* promoter. In other words, the Clp-mediated regulation of *manA* expression may be achieved in a cascade manner. A similar situation has also been found in Clp-regulated *prt1* (*51*).

A previous study has shown that mannanase activity cannot be detected in culture supernatant of *rpfF* mutant in Xcc strain 8004 grown in L medium (*12*). Recently, it has been demonstrated by microarray analysis of another Xcc strain, XC1, that (i) deletion of *clp* changes expression of 299 genes (*9*) and (ii) expression of 165 genes is affected by a mutation in *rpfF* (*13*). However, neither *manA* studied here nor another Clp and RpfF upregulated gene *pehA* (*22*) in Xcc strain Xc17 was included in the lists. In the above oligomicroarray study, it was shown that *manA* transcription was only slightly upregulated by DSF signals; hence, it was not included in the RpfF/DSF regulon in Xcc strain XC1 (*13*). In addition, deletion of *clp* in Xcc strain XC1 had no significant effect on *manA* transcription (*9*). Xcc strain-dependent variation in virulence has been documented (*14*). Thus, our findings that both Clp and RpfF positively regulate *manA* expression, demonstrated via both transcriptional fusion assay as well as extracellular mannanase activity analysis, together with the results of a previous study (*22*), suggest the existence of strain-dependent variations in the DSF signaling pathway including Clp and RpfF. In a more recent study, it was shown that, in addition to the DSF signaling system, the two-component regulatory system RavS/RavR regulates virulence gene expression through the global regulator Clp in Xcc strain XC1 (*53*). In that report, microarray analysis identified 245 RavR-regulated genes in XC1, among which 172 are also regulated by Clp while *manA* was absent from the list (*53*). Whether *manA* expression is RavS/RavR-dependent in Xc17 requires further study.

It was also noted that the β-galactosidase level in a culture of Xc17(pFY-362+52) increased following cell growth and continued increasing without leveling off at 30 h after entering the tationary phase (**Figure 2A**). A similar expression profile was found in the protease gene *prt1*, in which the transcription increased in the stationary phase (*51*). In addition, it was observed that the expression of *manA* is slightly induced (2.19-fold) in the presence of LBG (**Figure 2E** and **F**). Substrate-mediated induction of genes encoding extracellular enzymes in Xcc has also been documented, in which *prt1* or *pehA* was induced in the presence of its substrate, casein protein or polygalacturonic acid, respectively (*22*, *51*).

Properties of rManA. The optimal pH of rManA fell within the range of the values reported for other bacterial mannanases as shown in **Table 3**, although the optimal temperature was lower. It has been indicated that the pH optima of Man5A and Man5B of *C. japonicus* are between 7.5 and 8.0 (*43*). The ManA of *S. lividans* is active between 35 and 70 °C with an optimum at 58 °C and in a pH range of 5.5−8.0 with a maximum pH of 6.8 (*41*). In the case of *Vibrio* sp. MA-138 mannanase, it was found that purified ManA exhibits maximal activity at pH 6.5 and 40 °C (*54*). A more recent study indicated that Man5C, a second mannanase secreted by the same bacteria, exhibits maximal activity at 50 °C and pH 7.0 (*17*). From previously reported thermostability experiments, (i) the Man5A and Man5B of *C. japonicus* are stable up to 50 °C (*43*), (ii) the Man5C of *Vibrio* sp. MA-138 is stable up to 45 °C for 20 min (*17*), and (iii) mannanase from *Bacillus* sp. N16−5 is stable up to 60 °C during a 2-h incubation period and is unstable at temperatures of 60 °C (*55*). The latter is an alkaline mannanase purified from alkaliphilic *Bacillus* sp. N16-5 culture broth with optimum activity at pH 9.5 and 70 °C and more than 70% of the maximum activity detectable between pH 7 and 11 (*55*).

Microbial mannanases were affected differently by metal ions. Even the effects of Na^+, K^+, Ca^{2+}, and Mg^{2+} on ManA from *Vibrio* sp. MA-138 are not significant (ranging from 107% to 117%), and the mannanase activity is moderately inhibited by Mn^{2+} (48%) (*54*). However, the mannanase activity of ManA from *Bacillus* sp. N16-5 is slightly enhanced by Mg^{2+}, not affected by Ca^{2+}, and moderately inhibited by Mn^{2+} (36%) (*55*). The mannanase activity of *Vibrio* sp. MA-138 ManA is strongly inhibited by Ag^+, Cu^{2+}, Zn^{2+}, Hg^{2+}, and Fe^{3+} (*54*). In addition, Man5C from *Vibrio* sp. MA-138 is inhibited more than 80% by Ag^+, Cu^{2+}, Zn^{2+}, Hg^{2+}, and Al^{3+} (*17*). However, the activity of the mannanase from *Bacillus* sp. N16-5 is not affected by Cu^{2+} (*55*). Together with our results, it is shown that the effects of Mn^{2+} and Cu^{2+} on mannanase from different bacterial species are more diverse than those of other ions tested in these studies. For example, Xcc rManA is slightly enhanced by Mn^{2+} (109%), while both *Bacillus* sp. N16-5 and *Vibrio* sp. MA-138 ManAs are moderately inhibited (36% and 48%) by it (*54*, *55*). In addition, Xcc rManA and *Vibrio* sp. MA-138 ManA are strongly inhibited by Cu^{2+} (about 0−3%), while *Bacillus* sp. N16-5 ManA is not affected (105%) by this ion (*54*, *55*).

It has been shown that the biofilm dispersing activity of Xcc is insensitive to inhibition by 5 mM EDTA and several protease inhibitors (*12*). The data shown in **Table 2** also display similar resistance to 10 mM EDTA. However, mannanase from *Bacillus* sp. N16-5 is slightly inhibited by EDTA at 10 mM concentration (*55*). The ManA from *Vibrio* sp. MA-138 is also slightly inhibited by EDTA and iodoacetic acid both at 1 mM concentration (*54*). It is plausible that the EDTA effect on *Vibrio* sp. MA-138 ManA may be more pronounced at 10 mM concentration.

It has been reported that Trp residue(s) play an important part at the active site or the substrate binding site of manannase, as several microbial mannanases (from *Streptomyces* sp. strain no. 17, *Bacillus* sp. strain AM-001, *E. casseliflavus* FL2121, and *Vibrio* sp. MA-138) are completely inhibited by *N*-bromosuccinimide (*54*). Two conserved Trp residues whose putative role is involved in substrate binding in Xcc ManA (Trp^{54} and Trp^{278}, see below) do exist in *Vibrio* sp. MA-138 ManA (Trp^{49} and Trp^{273}). It is reasonable to predict that this chemical modifier, *N*-bromosuccinimide,

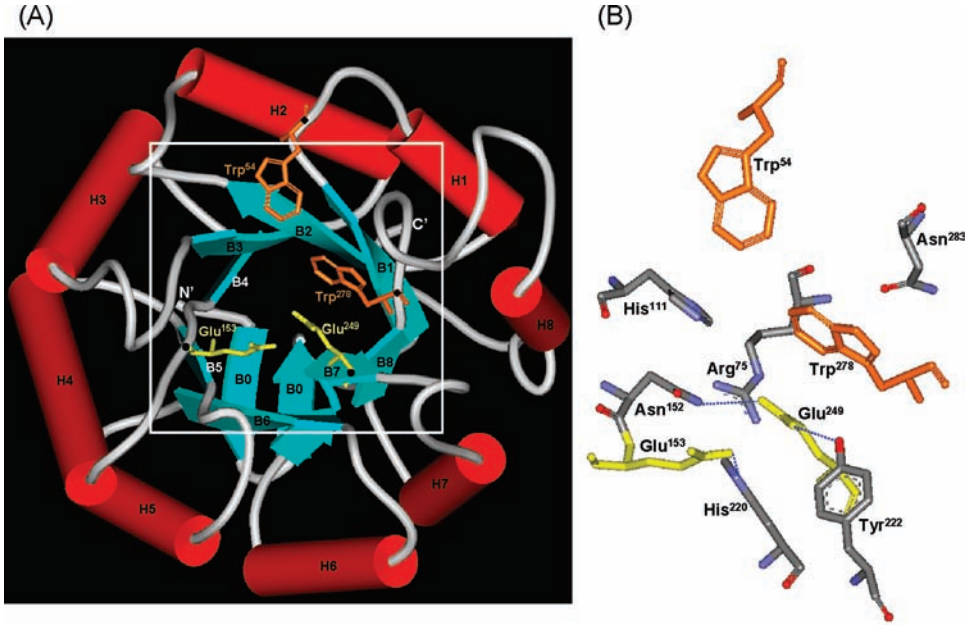

Figure 7. Model of 3-dimensional structure of Xcc ManA. (**A**) Schematic presentation of the structure of Xcc ManA. The two β-strands (B0), which form the bottom of the barrel motif and the other β-strands (B1 to B8), are shown as blue arrows. α-Helices (H1 to H8) are depicted as red cylinders. Catalytic and substrate stacking residues are numbered and shown as yellow and orange stick representations, respectively. The box presents the catalytic cleft of Xcc ManA. (**B**) Close-up view of the predicted catalytic site in a similar orientation as in part **A** in a stick and colored representation. Hydrogen-bonding interactions between backbone groups are marked as broken blue lines.

also inhibits rManA, although no experimental evidence has been obtained.

Comparatively little is known about the effects reducing agents as well as detergents exert on mannanase activity. It was known that the *Vibrio* sp. MA-138 ManA is not affected by dithiothreitol at 1 mM concentration (*54*). Apart from dithiothreitol, the Xcc rManA was also resistant to β-mercaptoethanol, Tween 20, and Triton X-100. There have been no reports documenting the effects of such reagents on mannanases in the GH5 family. The reason for the resistance is not clear.

Previous studies have indicated that external addition of DSF or mannanase-containing culture supernatant from wild-type Xcc triggers dispersion of the aggregates formed by the *rpfF* mutant (*11*−*13*). To test the effects of rManA on the dispersal of Xcc aggregate, purified rManA was added to bacterial cultures of different Xcc strains, and it was revealed that almost all of the bacteria including the RM17F were in the planktonic state (data not shown) after 5 min of treatment. These results indicated that, even with an extra 56 amino acids in its N-terminal, the purified rManA overexpressed from *E. coli* has compatible function to that produced in Xcc. This stretch of additional residue did not cause any detrimental effects on the mannanase activity. A possibility that cannot be ruled out is that the rManA with a 56 amino acids extension may serve a protective role, in which this recombinant protein has resistance to EDTA at higher concentration than that reported in ref *12* and is resistant to several reducing agents and detergents used in this study.

Kinetic comparisons of mannanases are difficult, since polymeric chains of mannose substituted with galactose, which are used as substrates, vary with the length and degree of substitution and are a function of the preparation method and the source of galactoman. The K_m value for the ACG substrate has been determined for the hyperthermophilic eubacterium *Thermotoga neapolitana* mannanase and reported to be 0.23 mg/mL (*56*). Although this suggests a lower affinity of substrate binding, side-by-side comparisons of the two enzymes on substrates prepared under identical conditions need to be done to verify this difference.

Predicted Structure of rManA. Secondary structure information shown in **Figure 6** indicated that the positions of predicted structural elements in Tfu Man, Bsp Man5A, and Bag Man5A coincided well with previous results assigned by X-ray crystallography (*44*−*46*). The catalytic domains of these proteins show the classical $(\alpha/\beta)_8$-barrel structure, similar to the catalytic domain of other enzymes in the GH5 family (*40*, *57*). It is reasonable to predict that Xcc ManA is also composed of a similar structure.

Based on the predicted α-helices and β-strands shown under each structure, eight α-helices and eight β-strands in the secondary structure assignment were constructed from the PDBsum database, and the 3-dimensional structure of Xcc ManA was built by homology modeling (**Figure 7A**). Xcc ManA might be structurally related to *T. fusca* β-mannanase and adopt the classical $(\alpha/\beta)_8$-barrel motif architecture contained in the catalytic domain of GH5 enzymes. Aside from the structural elements of the barrel, two short β strands (B0 shown here) at the N-terminus form the bottom of the barrel. The disulfide bond of *T. fusca* β-mannanase, between Cys^{74} and Cys^{81}, does not exist in the structure of Xcc ManA. Although Cys^{74} is conserved (at Cys^{99} in Xcc ManA), there is no counterpart for Cys^{81}, which is replaced by Ala^{106} in Xcc ManA.

From overall structural comparison with other GH5 enzymes, the catalytic functional significance of these key residues is clear. They all lie in and around the active site (**Figure 7B**) when using *T. fusca* β-mannanase for comparison (*44*). As shown in **Figures 6** and **7**, (i) Arg^{75} forms a putative salt bridge with Glu^{249} and a hydrogen bond with Asn^{152}; (ii) His^{111} together with Asn^{283} are equivalent to the putative substrate recognition; (iii) Asn^{152}, His^{220}, and Tyr^{222} maintain the positions of putative catalytic nucleophile in the active site environment through hydrogen bonding interactions; (iv) Glu^{153} and Glu^{249} perform the critical roles of putative acid/base catalyst donor and nucleophile catalyst of a GH5 enzyme, respectively; and (v) Trp^{278} together with Trp^{54} provide the putative hydrophobic stacking platforms for the sugar units in the substrate-binding sites.

One of the distinctive features of glycosyl hydrolases that attack the plant cell wall is that they generally contain noncatalytic modules that often bind to polysaccharide. These carbohydrate-binding modules (CBMs) have been classified into sequence-based families (see http://afmb.cnrs-mrs.fr/CAZY/index.html). Many family 5 mannanases have a modular structure consisting of a catalytic domain and noncatalytic CBMs, such as CBM10 found in Man5A and Man5B of *C. japonicus* (*43*), ManA of *S. lividans* and *Vibrio* sp. MA-138 (*41*, *42*); CBM2a found in Man5B of *C. japonicus* (*43*); and CBM27 found in Man5C of *Vibrio* sp. MA-138 (*17*) (**Table 3**). As shown in **Table 3**, inspection of the primary structure of the three *Xanthomonas* mannanases (encoded by *manA* in Xcc, *XAC1796* in *X. axonopodis* pv. citri, and *XCV1826* in *X. campestris* pv. vesicatoria) did not reveal any obvious linker sequences or protein motifs characteristic of the noncatalytic domains located in other family 5 mannanases. The mannanase in *Xanthomonas* is nonmodular, comprising a single catalytic domain.

In summary, the transcriptional regulation of *manA* gene encoding an extracellular mannanase of Xcc that is capable of dispersing aggregates was evaluated. In addition, the biofilm dispersal ability and biochemical properties of rManA produced by transformed *E. coli* were analyzed. Results have revealed that (i) the *manA* has its own promoter, (ii) Clp and RpfF positively regulate the expression of *manA*, (iii) the *manA* transcription is induced in the presence of LBG, (iv) the rManA produced by *E. coli* can disperse the aggregates formed by *rpfF* mutant, and (v) the rManA showed physical and biochemical characteristics similar to those of other mannanases belonging to the GH5 family even though no predictable CBM reported in this family was found in rManA. Thus, since no other reports have documented the transcription of *manA* as well as its gene product characterization, this appears to be the first study to characterize mannanase gene from *Xanthomans* spp. However, the true substrates of rManA await further investigation.

ABBREVIATIONS USED

AAP, Abridged Anchor Primer; ACG, azo-carob galactomannan; AUAP, Abridged Universal Amplification Primer; CBMs, carbohydrate-binding modules; Clp, cAMP receptor protein-like protein; DSF, diffusible signal factor; GH, glycosyl hydrolase; IPTG, isopropyl thio-β-D-galactoside; RACE, rapid amplification of cDNA ends; LBG, locust bean gum; rManA, recombinant ManA; Xcc, *Xanthomonas campestris* pv. campestris

LITERATURE CITED

(1) Williams, P. H. Black rot: A continuing threat to world crucifers. *Plant Dis.* **1980**, *64*, 736–742.

(2) Dow, J. M.; Daniels, M. J. Pathogenicity determinants and global regulation of pathogenicity of *Xanthomonas campestris* pv. campestris. *Curr. Top. Microbiol. Immunol.* **1994**, *192*, 29–41.

(3) Chan, J. W.; Goodwin, P. H. The molecular genetics of virulence of *Xanthomonas campestris*. *Biotechnol. Adv.* **1999**, *17*, 489–508.

(4) Wang, L.; Rong, W.; He, C. Two *Xanthomonas* extracellular polygalacturonases, PghAxc and PghBxc, are regulated by type III secretion regulators HrpX and HrpG and are required for virulence. *Mol. Plant-Microbe Interact.* **2008**, *21*, 555–63.

(5) Barber, C. E.; Tang, J. L.; Feng, J. X.; Pan, M. Q.; Wilson, T. J.; Slater, H.; Dow, J. M.; Williams, P.; Daniels, M. J. A novel regulatory system required for pathogenicity of *Xanthomonas campestris* is mediated by a small diffusible signal molecule. *Mol. Microbiol.* **1997**, *24*, 555–66.

(6) Slater, H.; Alvarez-Morales, A.; Barber, C. E.; Daniels, M. J.; Dow, J. M. A two-component system involving an HD-GYP domain protein links cell-cell signalling to pathogenicity gene expression in *Xanthomonas campestris*. *Mol. Microbiol.* **2000**, *38*, 986–1003.

(7) Wang, L. H.; He, Y.; Gao, Y.; Wu, J. E.; Dong, Y. H.; He, C.; Wang, S. X.; Weng, L. X.; Xu, J. L.; Tay, L.; Fang, R. X.; Zhang, L. H. A bacterial cell-cell communication signal with cross-kingdom structural analogues. *Mol. Microbiol.* **2004**, *51*, 903–12.

(8) He, Y. W.; Wang, C.; Zhou, L.; Song, H.; Dow, J. M.; Zhang, L. H. Dual signaling functions of the hybrid sensor kinase RpfC of *Xanthomonas campestris* involve either phosphorelay or receiver domain-protein interaction. *J. Biol. Chem.* **2006**, *281*, 33414–21.

(9) He, Y. W.; Ng, A. Y.; Xu, M.; Lin, K.; Wang, L. H.; Dong, Y. H.; Zhang, L. H. *Xanthomonas campestris* cell-cell communication involves a putative nucleotide receptor protein Clp and a hierarchical signalling network. *Mol. Microbiol.* **2007**, *64*, 281–92.

(10) Costerton, J. W.; Lewandowski, Z.; Caldwell, D. E.; Korber, D. R.; Lappin-Scott, H. M. Microbial biofilms. *Annu. Rev. Microbiol.* **1995**, *49*, 711–45.

(11) Crossman, L.; Dow, J. M. Biofilm formation and dispersal in *Xanthomonas campestris*. *Microbes Infect.* **2004**, *6*, 623–9.

(12) Dow, J. M.; Crossman, L.; Findlay, K.; He, Y. Q.; Feng, J. X.; Tang, J. L. Biofilm dispersal in *Xanthomonas campestris* is controlled by cell-cell signaling and is required for full virulence to plants. *Proc. Natl. Acad. Sci. U.S.A.* **2003**, *100*, 10995–1000.

(13) He, Y. W.; Xu, M.; Lin, K.; Ng, Y. J.; Wen, C. M.; Wang, L. H.; Liu, Z. D.; Zhang, H. B.; Dong, Y. H.; Dow, J. M.; Zhang, L. H. Genome scale analysis of diffusible signal factor regulon in *Xanthomonas campestris* pv. campestris: identification of novel cell-cell communication-dependent genes and functions. *Mol. Microbiol.* **2006**, *59*, 610–22.

(14) Qian, W.; Jia, Y.; Ren, S. X.; He, Y. Q.; Feng, J. X.; Lu, L. F.; Sun, Q.; Ying, G.; Tang, D. J.; Tang, H.; Wu, W.; Hao, P.; Wang, L.; Jiang, B. L.; Zeng, S.; Gu, W. Y.; Lu, G.; Rong, L.; Tian, Y.; Yao, Z.; Fu, G.; Chen, B.; Fang, R.; Qiang, B.; Chen, Z.; Zhao, G. P.; Tang, J. L.; He, C. Comparative and functional genomic analyses of the pathogenicity of phytopathogen *Xanthomonas campestris* pv. campestris. *Genome Res.* **2005**, *15*, 757–67.

(15) Vorholter, F. J.; Schneiker, S.; Goesmann, A.; Krause, L.; Bekel, T.; Kaiser, O.; Linke, B.; Patschkowski, T.; Ruckert, C.; Schmid, J.; Sidhu, V. K.; Sieber, V.; Tauch, A.; Watt, S. A.; Weisshaar, B.; Becker, A.; Niehaus, K.; Puhler, A. The genome of *Xanthomonas campestris* pv. campestris B100 and its use for the reconstruction of metabolic pathways involved in xanthan biosynthesis. *J. Biotechnol.* **2008**, *134*, 33–45.

(16) da Silva, A. C.; Ferro, J. A.; Reinach, F. C.; Farah, C. S.; Furlan, L. R.; Quaggio, R. B.; Monteiro-Vitorello, C. B.; Van Sluys, M. A.; Almeida, N. F.; Alves, L. M.; do Amaral, A. M.; Bertolini, M. C.; Camargo, L. E.; Camarotte, G.; Cannavan, F.; Cardozo, J.; Chambergo, F.; Ciapina, L. P.; Cicarelli, R. M.; Coutinho, L. L.; Cursino-Santos, J. R.; El-Dorry, H.; Faria, J. B.; Ferreira, A. J.; Ferreira, R. C.; Ferro, M. I.; Formighieri, E. F.; Franco, M. C.; Greggio, C. C.; Gruber, A.; Katsuyama, A. M.; Kishi, L. T.; Leite, R. P.; Lemos, E. G.; Lemos, M. V.; Locali, E. C.; Machado, M. A.; Madeira, A. M.; Martinez-Rossi, N. M.; Martins, E. C.; Meidanis, J.; Menck, C. F.; Miyaki, C. Y.; Moon, D. H.; Moreira, L. M.; Novo, M. T.; Okura, V. K.; Oliveira, M. C.; Oliveira, V. R.; Pereira, H. A.; Rossi, A.; Sena, J. A.; Silva, C.; de Souza, R. F.; Spinola, L. A.; Takita, M. A.; Tamura, R. E.; Teixeira, E. C.; Tezza, R. I.; Trindade dos Santos, M.; Truffi, D.; Tsai, S. M.; White, F. F.; Setubal, J. C.; Kitajima, J. P. Comparison of the genomes of two *Xanthomonas* pathogens with differing host specificities. *Nature* **2002**, *417*, 459–63.

(17) Tanaka, M.; Umemoto, Y.; Okamura, H.; Nakano, D.; Tamaru, Y.; Araki, T. Cloning and characterization of a beta-1,4-mannanase 5C possessing a family 27 carbohydrate-binding module from a marine bacterium, *Vibrio* sp. strain MA-138. *Biosci. Biotechnol. Biochem.* **2009**, *73*, 109–16.

(18) Yoon, K. H.; Chung, S.; Lim, B. L. Characterization of the *Bacillus subtilis* WL-3 mannanase from a recombinant *Escherichia coli*. *J. Microbiol.* **2008**, *46*, 344–9.

(19) Hanahan, D. Studies on transformation of *Escherichia coli* with plasmids. *J. Mol. Biol.* **1983**, *166*, 557–80.

(20) Yang, B. Y.; Tseng, Y. H. Production of exopolysaccharide and levels of protease and pectinase activity in pathogenic and nonpathogenic strains of *Xanthomonas campestris* pv. campestris. *Bot. Bull. Acad. Sin.* **1988**, *29*, 93–99.

(21) Tseng, Y. H.; Choy, K. T.; Hung, C. H.; Lin, N. T.; Liu, J. Y.; Lou, C. H.; Yang, B. Y.; Wen, F. S.; Weng, S. F.; Wu, J. R. Chromosome map of *Xanthomonas campestris* pv. campestris 17 with locations of genes involved in xanthan gum synthesis and yellow pigmentation. *J. Bacteriol*. **1999**, *181*, 117–25.
(22) Hsiao, Y. M.; Zheng, M. H.; Hu, R. M.; Yang, T. C.; Tseng, Y. H. Regulation of the *pehA* gene encoding the major polygalacturonase of *Xanthomonas campestris* by Clp and RpfF. *Microbiology* **2008**, *154*, 705–13.
(23) Miller, J. H. *Experiments in Molecular Genetics*; Cold Spring Harbor Laboratory: Cold Spring Harbor, NY, 1972.
(24) Fu, J. F.; Tseng, Y. H. Construction of lactose-utilizing *Xanthomonas campestris* and production of xanthan gum from whey. *Appl. Environ. Microbiol*. **1990**, *56*, 919–23.
(25) Sambrook, J.; Fritsch, E. F.; Maniatis, T. *Molecular Cloning: a Laboratory Manual*, 2nd ed.; Cold Spring Harbor Laboratory: Cold Spring Harbor, NY, 1989.
(26) Hsiao, Y. M.; Liao, H. Y.; Lee, M. C.; Yang, T. C.; Tseng, Y. H. Clp upregulates transcription of *engA* gene encoding a virulence factor in *Xanthomonas campestris* by direct binding to the upstream tandem Clp sites. *FEBS Lett*. **2005**, *579*, 3525–33.
(27) Sanger, F.; Nicklen, S.; Coulson, A. R. DNA sequencing with chain-terminating inhibitors. *Proc. Natl. Acad. Sci. U.S.A*. **1977**, *74*, 5463–7.
(28) Wang, T. W.; Tseng, Y. H. Electrotransformation of *Xanthomonas campestris* by RF DNA of filamentous phage ϕLf. *Lett. Appl. Microbiol*. **1992**, *14*, 65–8.
(29) Frohman, M. A. Rapid amplification of complementary DNA ends for generation of full-length complementary DNAs: thermal RACE. *Methods Enzymol*. **1993**, *218*, 340–56.
(30) Lee, T. C.; Chen, S. T.; Lee, M. C.; Chang, C. M.; Chen, C. H.; Weng, S. F.; Tseng, Y. H. The early stages of filamentous phage ϕLf infection require the host transcription factor, Clp. *J. Mol. Microbiol. Biotechnol*. **2001**, *3*, 471–81.
(31) Bourgault, R.; Bewley, J. D. Gel diffusion assays for endo-beta-mannanase and pectin methylesterase can underestimate enzyme activity due to proteolytic degradation: a remedy. *Anal. Biochem*. **2002**, *300*, 87–93.
(32) McCleary, B. V. A simple assay procedure for beta-D-mannanase. *Carbohydr. Res*. **1978**, *67*, 213–21.
(33) Laemmli, U. K. Cleavage of structural proteins during the assembly of the head of bacteriophage T4. *Nature* **1970**, *227*, 680–5.
(34) Bradford, M. M. A rapid and sensitive method for the quantitation of microgram quantities of protein utilizing the principle of protein-dye binding. *Anal. Biochem*. **1976**, *72*, 248–54.
(35) Vieira, J.; Messing, J. New pUC-derived cloning vectors with different selectable markers and DNA replication origins. *Gene* **1991**, *100*, 189–94.
(36) Schweizer, H. D. Small broad-host-range gentamycin resistance gene cassettes for site-specific insertion and deletion mutagenesis. *Biotechniques* **1993**, *15*, 831–4.
(37) Keen, N. T.; Tamaki, S.; Kobayashi, D.; Trollinger, D. Improved broad-host-range plasmids for DNA cloning in gram-negative bacteria. *Gene* **1988**, *70*, 191–7.
(38) Nielsen, H.; Engelbrecht, J.; Brunak, S.; von Heijne, G. Identification of prokaryotic and eukaryotic signal peptides and prediction of their cleavage sites. *Protein Eng*. **1997**, *10*, 1–6.
(39) Thieme, F.; Koebnik, R.; Bekel, T.; Berger, C.; Boch, J.; Buttner, D.; Caldana, C.; Gaigalat, L.; Goesmann, A.; Kay, S.; Kirchner, O.; Lanz, C.; Linke, B.; McHardy, A. C.; Meyer, F.; Mittenhuber, G.; Nies, D. H.; Niesbach-Klosgen, U.; Patschkowski, T.; Ruckert, C.; Rupp, O.; Schneiker, S.; Schuster, S. C.; Vorholter, F. J.; Weber, E.; Puhler, A.; Bonas, U.; Bartels, D.; Kaiser, O. Insights into genome plasticity and pathogenicity of the plant pathogenic bacterium *Xanthomonas campestris* pv. vesicatoria revealed by the complete genome sequence. *J. Bacteriol*. **2005**, *187*, 7254–66.
(40) Davies, G.; Henrissat, B. Structures and mechanisms of glycosyl hydrolases. *Structure* **1995**, *3*, 853–9.
(41) Arcand, N.; Kluepfel, D.; Paradis, F. W.; Morosoli, R.; Shareck, F. Beta-mannanase of *Streptomyces lividans* 66: cloning and DNA sequence of the *manA* gene and characterization of the enzyme. *Biochem. J*. **1993**, *290* (*Pt 3*), 857−63.
(42) Tamaru, Y.; Araki, T.; Morishita, T.; Kimura, T.; Sakka, K.; Ohmiya, K. Cloning, DNA sequencing, and expression of the β-1,4-mannanase gene from a marine bacterium, *Vibrio* sp. strain MA-138. *J. Ferment Bioeng*. **1997**, *83*, 201–5.
(43) Hogg, D.; Pell, G.; Dupree, P.; Goubet, F.; Martin-Orue, S. M.; Armand, S.; Gilbert, H. J. The modular architecture of *Cellvibrio japonicus* mannanases in glycoside hydrolase families 5 and 26 points to differences in their role in mannan degradation. *Biochem. J*. **2003**, *371*, 1027–43.
(44) Hilge, M.; Gloor, S. M.; Rypniewski, W.; Sauer, O.; Heightman, T. D.; Zimmermann, W.; Winterhalter, K.; Piontek, K. High-resolution native and complex structures of thermostable beta-mannanase from *Thermomonospora fusca*—substrate specificity in glycosyl hydrolase family 5. *Structure* **1998**, *6*, 1433–44.
(45) Akita, M.; Takeda, N.; Hirasawa, K.; Sakai, H.; Kawamoto, M.; Yamamoto, M.; Grant, W. D.; Hatada, Y.; Ito, S.; Horikoshi, K. Crystallization and preliminary X-ray study of alkaline mannanase from an alkaliphilic *Bacillus* isolate. *Acta Crystallogr., D: Biol. Crystallogr*. **2004**, *60*, 1490–2.
(46) Tailford, L. E.; Ducros, V. M.; Flint, J. E.; Roberts, S. M.; Morland, C.; Zechel, D. L.; Smith, N.; Bjornvad, M. E.; Borchert, T. V.; Wilson, K. S.; Davies, G. J.; Gilbert, H. J. Understanding how diverse -mannanases recognise heterogeneous substrates. *Biochemistry*, in press.
(47) Sakon, J.; Adney, W. S.; Himmel, M. E.; Thomas, S. R.; Karplus, P. A. Crystal structure of thermostable family 5 endocellulase E1 from *Acidothermus cellulolyticus* in complex with cellotetraose. *Biochemistry* **1996**, *35*, 10648–60.
(48) Katzen, F.; Becker, A.; Zorreguieta, A.; Puhler, A.; Ielpi, L. Promoter analysis of the *Xanthomonas campestris* pv. campestris *gum* operon directing biosynthesis of the xanthan polysaccharide. *J. Bacteriol*. **1996**, *178*, 4313–8.
(49) de Crecy-Lagard, V.; Glaser, P.; Lejeune, P.; Sismeiro, O.; Barber, C. E.; Daniels, M. J.; Danchin, A. A *Xanthomonas campestris* pv. campestris protein similar to catabolite activation factor is involved in regulation of phytopathogenicity. *J. Bacteriol*. **1990**, *172*, 5877–83.
(50) Hsiao, Y. M.; Fang, M. C.; Sun, P. F.; Tseng, Y. H. Clp and RpfF up-regulate transcription of *pelA1* gene encoding the major pectate lyase in *Xanthomonas campestris* pv. campestris. *J. Agric. Food Chem*. **2009**, *57*, 6207–15.
(51) Hsiao, Y. M.; Tseng, Y. H. Transcription of *Xanthomonas campestris prt1* gene encoding protease 1 increases during stationary phase and requires global transcription factor Clp. *Biochem. Biophys. Res. Commun*. **2002**, *295*, 43–9.
(52) Dong, Q.; Ebright, R. H. DNA binding specificity and sequence of *Xanthomonas campestris* catabolite gene activator protein-like protein. *J. Bacteriol*. **1992**, *174*, 5457–61.
(53) He, Y. W.; Boon, C.; Zhou, L.; Zhang, L. H. Co-regulation of *Xanthomonas campestris* virulence by quorum sensing and a novel two-component regulatory system RavS/RavR. *Mol. Microbiol*. **2009**, *71*, 1464–76.
(54) Tamaru, Y.; Araki, T.; Amagoi, H.; Mori, H.; Morishita, T. Purification and characterization of an extracellular beta-1,4-mannanase from a marine bacterium, *Vibrio* sp. strain MA-138. *Appl. Environ. Microbiol*. **1995**, *61*, 4454–8.
(55) Ma, Y.; Xue, Y.; Dou, Y.; Xu, Z.; Tao, W.; Zhou, P. Characterization and gene cloning of a novel beta-mannanase from alkaliphilic *Bacillus* sp. N16-5. *Extremophiles* **2004**, *8*, 447–54.
(56) Duffaud, G. D.; McCutchen, C. M.; Leduc, P.; Parker, K. N.; Kelly, R. M. Purification and characterization of extremely thermostable beta-mannanase, beta-mannosidase, and alpha-galactosidase from the hyperthermophilic eubacterium *Thermotoga neapolitana* 5068. *Appl. Environ. Microbiol*. **1997**, *63*, 169–77.
(57) Henrissat, B. A classification of glycosyl hydrolases based on amino acid sequence similarities. *Biochem. J*. **1991**, *280* (*Pt 2*), 309−16.

Received for review October 16, 2009. Revised manuscript received December 16, 2009. Accepted December 29, 2009. Y.-F.L. and M.-C.F. contributed equally to this study. This study was supported by grants from the National Science Council, Republic of China (NSC95-2313-B-166-005 and NSC96−2313-B-166−003).